JCTC Journal of Chemical Theory and Computation

Probing Membrane Insertion Activity of Antimicrobial Polymers via Coarse-Grain Molecular Dynamics

Carlos F. Lopez,[†] Steven O. Nielsen,[†] Goundla Srinivas,[†] William F. DeGrado,[‡] and Michael L. Klein*[,†]

Center for Molecular Modeling, Department of Chemistry, University of Pennsylvania, 231 South 34th Street, Philadelphia, Pennsylvania 19104-6323, and Department of Biochemistry and Biophysics, University of Pennsylvania School of Medicine, Philadelphia, Pennsylvania 19104-6059

Received November 30, 2005

Abstract: Knowledge of the mechanism of action of antimicrobial agents is crucial for the development of new compounds to combat microbial pathogens. To this end, computational studies on the interaction of known membrane-active antimicrobial polymers with phospholipid bilayers reveal spontaneous membrane insertion and cooperative action at low and high concentrations, respectively. In late-stage attack, antimicrobials cross the membrane core and occasionally align to provide a stepping-stone pathway for water permeation; this suggests a possible new mode of action that does not depend on pore formation for transport to and across the inner leaflet. The computations rationalize the observed activity of a new class of antimicrobial compounds.

Introduction

The emergence of new bacteria and viruses,[1,2] increasing pathogen resistance to treatment,[3] and the threat of bioterrorism[4] underscore the vital need to understand the mechanisms of action of antimicrobial molecules. For these reasons, renewed interest in generic classes of antigenic therapeutic agents[5−11] has led to synthetic designs which show great potential for combating infectious pathogens. Indeed, nonpeptidic synthetic antimicrobials show promise as effective alternatives to their natural peptide counterparts.[12] Some advantages include lower cost of manufacturing and the fact that synthetic molecules are more resistant to degradation by the host organism. Various mechanisms of action have been proposed for membrane-targeting antimicrobials. Although no general mechanism of action has been established even for cationic peptides, the commonly accepted Shai-Matsuzaki-Huang model provides a reasonable explanation for the observed antimicrobial activity of such compounds.[6,13,14] A number of molecules exist, however, that do not seem to completely follow this model in their mechanism of action.[15,16]

Motivating the work presented here is a desire to understand the nature of poration caused by synthetic antimicrobial (AM) molecules interacting with a phospholipid membrane. The specific AM molecule considered is the amphipathic aryl amide dimer (Figure 1), which has been shown to have potent antimicrobial activity and was inspired by natural and synthetic peptides.[6,10,12,17] It was shown experimentally that arylamide polymers, at different concentrations, act as bactericidal agents.[12] Their interaction with the membrane was established by the measurement of AM induced calcein leakage from large unilamellar vesicles. Here, we report the results of coarse grained (CG) molecular dynamics (MD) simulations of a fully hydrated 256 dimyristoyl-phosphatidylcholine (DMPC) lipid bilayer in the presence of 0, 1, 2, 8, or 18 AM molecules, to assess concentration dependent effects on the membrane. Although the bulk concentration is known experimentally, the two-dimensional concentration of antimicrobials at the surface is not known. For this reason we probe the antimicrobial-membrane relation at different concentrations. These concentrations were chosen to be

* Corresponding author e-mail: klein@lrsm.upenn.edu.
[†] University of Pennsylvania.
[‡] University of Pennsylvania School of Medicine.

10.1021/ct050298p CCC: $33.50
Published on Web 03/24/2006

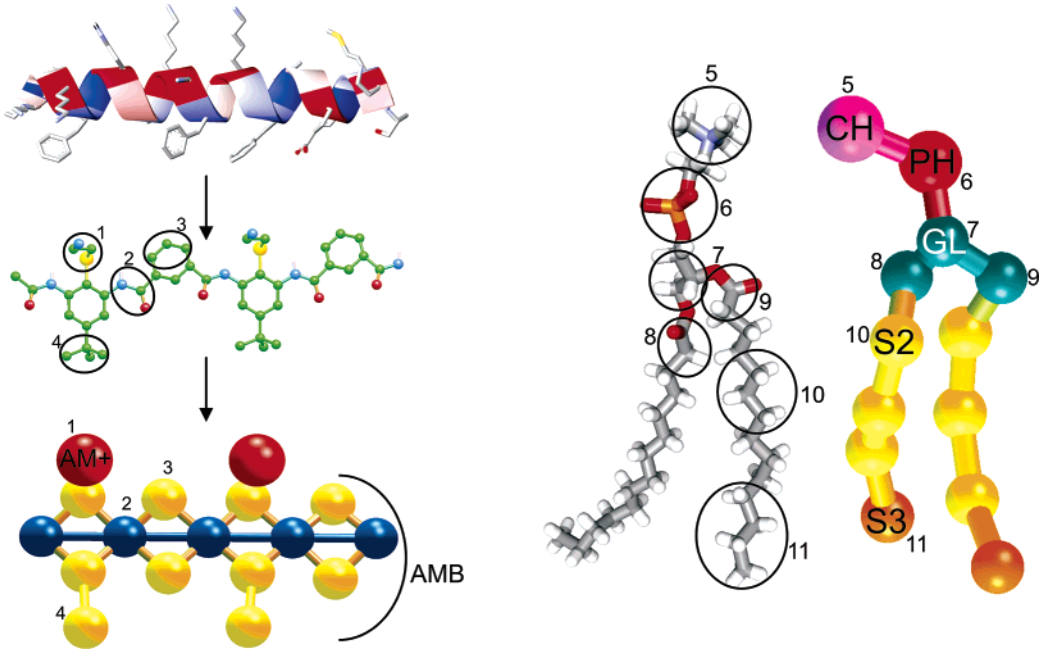

Figure 1. Inspiration for the design of synthetic antimicrobial targets and the coarse grain model used in the present simulations. Left: Ribbon representation of magainin, a potent natural antimicrobial. The α-helix ribbon is colored by hydrophobicity (red=hydrophobic, blue=hydrophilic), and selected individual amino acids are shown as sticks. Middle: The aryl amide dimeric polymer, a purely synthetic molecule inspired by natural antimicrobials. Color code: carbon, green; sulfur, yellow; oxygen, red; nitrogen, blue; hydrogen, white. Bottom: A coarse grain representation of the aryl amide dimeric polymer. Color code: cationic, red; peptidic, blue; hydrophobic, yellow. Right: The corresponding units between an all atom DMPC molecule (left) and its CG representation (right). Color code: nitrogen, blue; carbon, gray; oxygen, red; phosphate, orange; hydrogen, white. CG color code: choline (CH), purple; phosphate (PH), red; glycerol (GL), blue-gray; alkane (S2), yellow; terminal alkane (S3), orange. Circles in the atomistic representations correspond to the numbered units in the coarse grain representations.

similar to those observed by Huang in experiments with membrane-active peptides.[7]

Molecular dynamics (MD) computer simulations provide a powerful complement to experiments on biological systems,[18,19] but to date attempts to explore the interactions of antimicrobials with membranes have probed only relatively short-time behavior[20] (10 ns or so) and few have included more than one membrane-active molecule.[21] There is a lack of quantitative information due to the difficulty in simulating events that span the relevant range of time scales for the host membrane, which is a sluggish partially ordered liquid−crystalline system. Modern coarse grain (CG) work, inspired by the pioneering efforts of Smit and co-workers,[22] has resulted in the development of several models for membrane simulations in the past years.[23,24] Such advances in methodology have allowed access to unprecedented time scales in MD simulations, extending them toward biologically relevant time scales.[25] The longest simulation in this work, effectively 2 μs, would be difficult to run using all-atom interaction potentials, with current algorithms and computational resources.[26] Using CG methods it is now possible to systematically explore events in this temporal regime.

Methods

CG Model. Reduced representations for water, alkane, phospholipids, and the arylamide based antimicrobial are used in the present work. The model is shown in detail in Figure 1, with labels which will be referenced throughout the manuscript. The model consists of units that represent collections of atoms which are tuned to mimic some key physical or structural features known from experiment or atomistic simulation as shown in Figure 1a,b. The basic model and current developments are described in detail in our earlier papers.[23,25,27] Briefly, single spherical sites represent triplets of alkane carbon atoms and their accompanying hydrogen atoms (S2 and S3 units). The hydrocarbon sites are linked together to form chains using stretching and bending potentials. Single spherical sites also represent triplets of water molecules (WS, not shown). The headgroup units are chosen so that the choline (CH) unit is represented by one site, the phosphate (PH) unit by one site, and the glycerol (GL), along with the accompanying carboxylic acids (EST, not labeled in Figure 1 for clarity), by three sites. Several existing units were used to build the arylamide antimicrobial.[12] The positively charged section was approximated using an existing choline site (AM+), which is similar to the group we are trying to emulate. The remainder of the antimicrobial was modeled using generic hydrophobic sites (S2, S3 where appropriate), and carboxylic sites (EST) from the original model in an effort to preserve both the hydrophobic and slightly hydrophilic character of the antimicrobial bonds and the benzene ring. Special care was taken to preserve the overall size and shape of the arylamide molecules in the coarse grain construct.

One of the most important advantages of this approach is the effective increase in simulation times when compared to an equivalent all-atom molecular dynamics simulation. With the present model we observe an increase in time

efficiency of about 4 orders of magnitude,[25] currently allowing access to microsecond phenomena employing modest computational resources. In the present paper we report effective simulation times for each simulation. We have used the lateral lipid diffusion of the CG membrane and compared this to the CG lateral diffusion of an all-atom membrane. The two-dimensional lateral diffusion constant for the L_α phase of DMPC in the plane of the bilayer is 6.5×10^{-8} cm^2 s^{-1} for an all-atom simulation and 6.3×10^{-6} cm^2 s^{-1} for the CG model. The CG lipid motions are therefore 2 orders of magnitude faster than their all-atom counterparts. We use a factor of 1×10^2 to recalibrate the simulation time evolution and account for the molecular diffusion speedup. The effective simulation times reported in the paper therefore reflect this correction.

Simulation. All the simulations presented in this paper were run using our in-house CM3D molecular dynamics program. The program can perform calculations with full electrostatics, multiple time-step integrators following the RESPA[28] technique, and a wide variety of ensembles ranging from microcanonical (NVE) to isobaric-isothermic (NPT). The simulations contained in the present report were all run using the NPT ensemble at 303 K temperature and 1 atm pressure in an orthorhombic simulation cell with flexible sides. The temperature and pressure were controlled with the Nosé-Hoover chain methodology.[29] The outer simulation time step was chosen at 10 fs using a multiple time step algorithm.

Five simulations are reported in this work containing 0, 1, 2, 8, and 18 antimicrobial molecules, placed in close proximity (but outside) of a 256 DMPC hydrated lipid bilayer, which was constructed as described previously.[25] The simulations were run for 204 ns, 86 ns, 160 ns, 160 ns, and 1.9 μs effective simulation time (referred to throughout the text as AM0, AM1, AM2, AM8, and AM18, respectively). With the present model these simulations, for the longest run system, can be run on a high end Intel based single-processor workstation within a few weeks.

Analysis. The atom weighted density profiles were calculated by constructing a histogram along the axis perpendicular to the bilayer plane of each CG unit. Each unit was then weighted by the number of electrons of its corresponding all-atom counterpart (e.g. 42 electrons for the S2 site representing $(-CH_2-)_3$). The electron weight was then distributed along the histogram using a Gaussian function with a width corresponding to the Lennard-Jones radius of the CG unit. Given the nonequilibrium nature of the present simulations, the first quarter of the simulations was not included in the calculation of the atom weighted density profiles for simulations with 1, 2, and 8 AM, as shown in Figure 4. The first 50 ns of the 18 AM simulation were skipped. The next 150 ns were processed to obtain the data presented in Figure 4. The last 200 ns of the 18 AM simulation were used to generate the data presented in Figure 5.

Water transport across the bilayer was assessed by an algorithm written to monitor water molecules that cross the plane defined by the glycerol units on either bilayer leaflet. A water unit was counted once it crossed both glycerol planes passing across the bilayer core. Despite the length of the simulation water crossing is still a rare event. We simply divide the number of crossing waters by the simulation time after half of the AM molecules flip-flop across the core of the membrane to obtain a rough estimate of the qualitative passage rate.

The molecule insertion coordinate was calculated by obtaining the average *z*-axis coordinate between the end peptidic units (labeled "3" in Figure 1). The *z*-axis was defined as the axis perpendicular to the membrane plane, with the zero of the axis set to the center of the bilayer. As a visual aid, lines representing the average position of the choline groups and the glycerol groups were placed on the graphs for reference. Similarly the insertion angles were determined by obtaining the angle between the end peptidic units and the bilayer normal, which was approximated, in this case, as the *z*-axis.

Results and Discussion

Insertion Mechanism. We observe spontaneous insertion of antimicrobial polymers in all of the antimicrobial containing simulations reported here (Figure 2). It appears that cooperative activity occurs at high AM concentrations, as one molecule possesses the capacity to interact with and assist penetration of other AMs into the lipid bilayer. In the early stages of the simulation the AM molecules accumulate at the headgroup region of the outer leaflet lipid−water interface (Figure 2a) with their hydrophilic amide groups in the water. As the simulation evolves the AM molecules dive into the membrane to reside under the lipid headgroups (Figure 2b). At still longer times, as observed in the 18 AM simulation, some AM molecules cross the lipid bilayer core to reside under the headgroups of the inner leaflet (Figure 2c).

We have rationalized our observations by postulating the existence of two AM insertion mechanisms. The first consists of the spontaneous penetration of single, isolated AM molecules (1 AM simulation), which is relevant at lower concentrations. Data for the distance from the AM molecule to the center of the bilayer as well as the orientation of the AM relative to the bilayer plane is shown in Figure 3. The dashed lines show the average position of the lipid CH (∼18 Å) and GL (∼13 Å) groups throughout the simulation. The insertion distance decreases as the simulation evolves, with the molecule center crossing the CH-GL slab in about 15 ns of simulation time (Figure 3a). At this point, once the molecule has crossed the GL region there is further accommodation and reorientation. The AM+ groups, as will be shown below, remain near the headgroup region, while the body of the AM intercalates between the lipid tails. As shown in Figure 3b, the orientation of the molecule throughout the insertion is almost parallel to the membrane plane. This mechanism of insertion seems to indicate a simple spontaneous insertion at low concentrations for the antimicrobial. We are currently working on ways to characterize the insertion time scale for this event.

In addition to the previously described mechanism of insertion, a second mechanism is seen when AM molecules interact. To probe the latter, several simulations (2 AM, 8

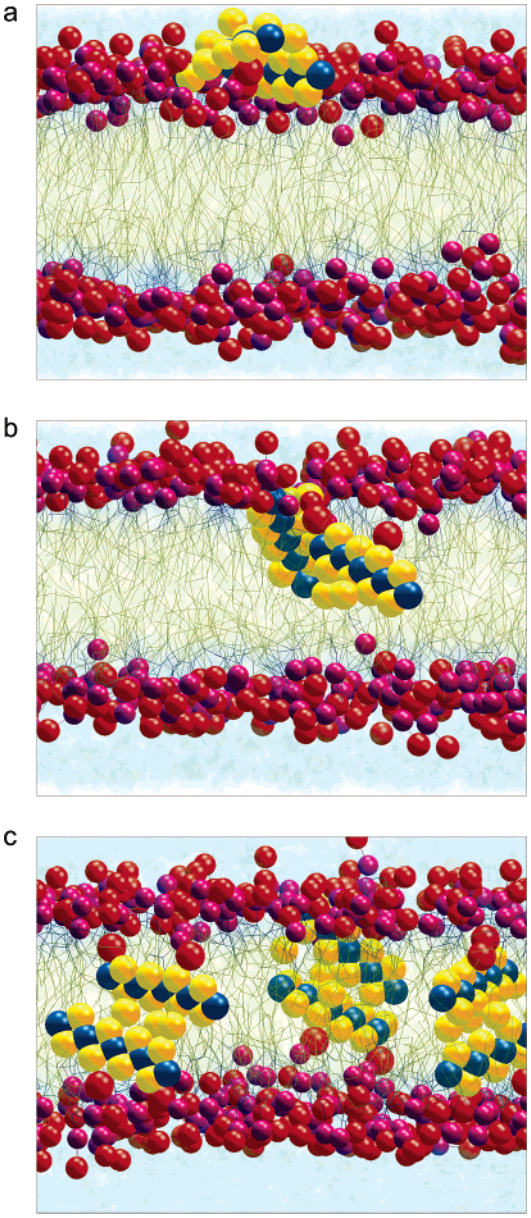

Figure 2. Depiction of the observed two-step - accommodation (a) and penetration (b) mechanism for membrane insertion of the antimicrobial (AM) aryl amide dimer molecules into the outer leaflet of a DMPC lipid bilayer (DMPC: choline, red; phosphate, purple; glycerol group, blue sticks; hydrophobic tails, green sticks). The initial interfacial insertion stage involves adsorption and "snorkeling" of the AM at the bilayer surface (a). In this example of the penetration stage, one AM rotates to become perpendicular to the bilayer plane and drags the accompanying AM into the membrane core (b). Subsequent population of both leaflets occurs at much longer times (c).

AM, and 18 AM) were initiated with AM molecules in close proximity relative to each other and wholly within the water subphase. The AM long axes were positioned parallel to the lipid membrane, and all the AM molecules were initially placed completely in the water subphase. We present the insertion distance and orientation angle for both AM molecules during insertion observed in the 2 AM simulation, shown in Figure 3c,d. Both antimicrobials initially approach the membrane and accommodate near the headgroup region as shown in Figure 2a. Figure 3c shows how the centers of the AM molecules approach the bilayer at about the same distance and time. It is important to note here that there is "contact" between the AMs throughout the insertion process. Within a short time of accommodation within the lipid headgroup region, one of the antimicrobials (labeled 2AM1 in Figure 3c) very rapidly changes orientation (Figure 3d). This antimicrobial will conserve this steep angle and its interaction with the second antimicrobial, which remains relatively parallel to the membrane throughout the insertion process. After this change in orientation, 2AM1 penetrates the membrane rather quickly. During this process it continues to interact with the second antimicrobial (2AM2) and "drags" it through the CH-GL region. After the groups have crossed the headgroup region dissociation between the two AMs occur and a shallower angle relative to the bilayer plane is recovered.

Eventually all of the arylamide monomers penetrate the membrane at sufficient time scales. Interfacial insertion times, throughout the simulations, were about 12 ns, and penetration times ranged from 10 to 20 ns throughout the different concentration simulations. About 50% of the AMs insert into the membrane via an accommodation/penetration mechanism as described here. The remaining 50% of the molecules are dragged into the bilayer core by those that experience a two stage mechanism. Further simulation might be required to extract proper time scales related to the accommodation and insertion events. The insertion and penetration mechanism observed in this study expands and adds pictorial detail to the traditional view of aggregation and oligomerization attributed to natural AM peptides such as magainins and melittins.[6,7,13,14] We are currently working on understanding how the cooperative interaction between AM molecules could be related to experimentally observed activity.

Membrane Structure. Figure 4 shows the results depicting the positions of the different protein components along the *z*-axis immediately after penetration of the membrane leaflet, nearest the side of attack, has taken place. The data analyzed here corresponds to the total simulation time for 0 AM, 1 AM, 2 AM, and 8 AM simulations and to about 200 ns of simulation time for the 18 AM simulation. As can be seen (Figure 4a), the membrane density on the side of attack decreases and broadens as the concentration increases. This is indicative of a displacement of the lipid headgroups due to the insertion of the AM polymers into the protein. There seems to be a decrease in the water density on the side of attack as the concentration increases as well. This is due, at least in part, to the antimicrobial molecules displacing water molecules at the lipid headgroup region. As shown by the dashed lines (Figure 4b), corresponding to the AM polymers, the AM+ units reside near the GL group of the lipid and between the GL and CH groups of the lipid. The body of the AM polymers however sits well past the GL groups. In the low concentration case a peak appears near the center of the bilayer. At higher concentrations, the distribution is broader, and the AM groups span several Ångstroms between the GL groups and parts of the opposite side of the lipid membrane. After insertion/penetration, the AM+ groups

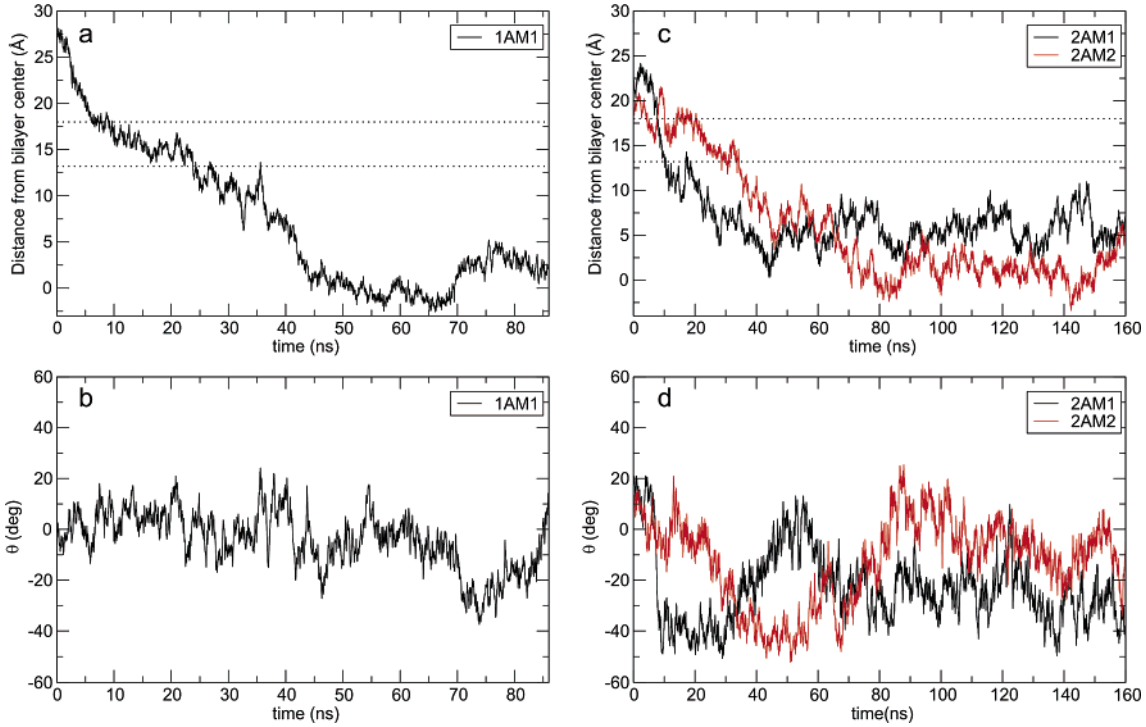

Figure 3. Insertion distance to bilayer center (top graphs) and orientation angle (bottom graphs) for the 1AM simulation (left) and the 2AM simulation (right). Dashed lines represent the average positions of the CH group (top line) and the GL group (bottom line) within the attacked leaflet.

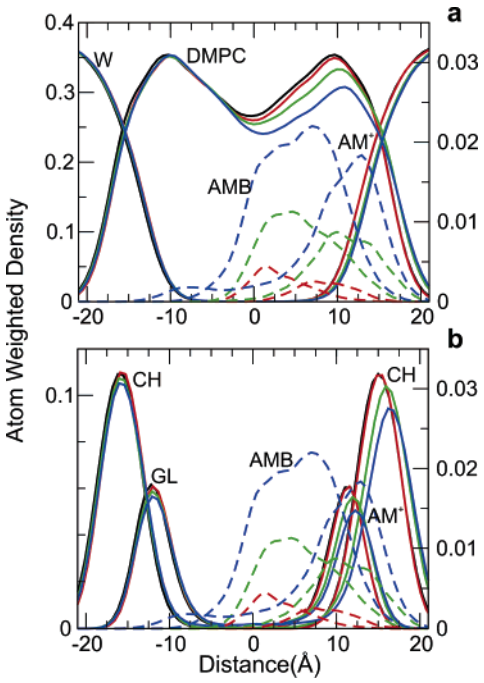

Figure 4. Atom weighted densities for the lipid bilayer (solid lines) and the AM molecules (dashed lines) for simulations with 0 (black), 2 (red), 8 (green), and 18 (blue) antimicrobial molecules. The scale on the left corresponds to the lipid molecules, while the scale on the right corresponds to the AM polymers.

reside close to the glycerol moieties, while the remainder of the molecule resides in the hydrophobic core.

At sufficiently long times all the AM molecules eventually insert into the membrane core and become oriented with their long axes parallel to the membrane surface. AM associations during the initial insertion process are lost via diffusion after further penetration into the membrane. After about 1 μs of simulation time, half of the AM polymers spontaneously cross the bilayer core and sit opposite the attack leaflet (18 AM simulation). The atom weighted densities showing the membrane structure are shown in Figure 5. At long times, there seems to be a preference for the AM body (labeled AMB in Figure 5a,b) to sit wholly near the center of the lipid membrane. The AM+ groups seem to prefer a position slightly below the GL groups (Figure 5b). This is in contrast to that observed initially after insertion where the AM+ group sits between the GL and CH groups. We believe this is due to transbilayer interactions with both lipids and other antimicrobial molecules. Indeed, as we will discuss below, AMs in one leaflet can interact and align with AMs from the opposite leaflet.

Typically, thinning of the system occurs when AM molecules are added to a hydrated lipid bilayer.[30] In the present simulations the membrane surface area (simulation cell cross section) increases slightly (6% at the highest concentration) and the overall system thickness (simulation cell height) decreases slightly (1% at the highest concentration) with increasing number of AMs.

Water Penetration and Transport. A decrease in water penetration at the attacked bilayer leaflet and an increase in water penetration at the leaflet opposite the AM attack are observed in the simulations. As AMs snorkel and dive through the membrane headgroup region they exclude water that normally resides at the interface. The leaflet opposite the AM attack expands in response to the swelling of the attacked leaflet, thereby enabling water penetration. This

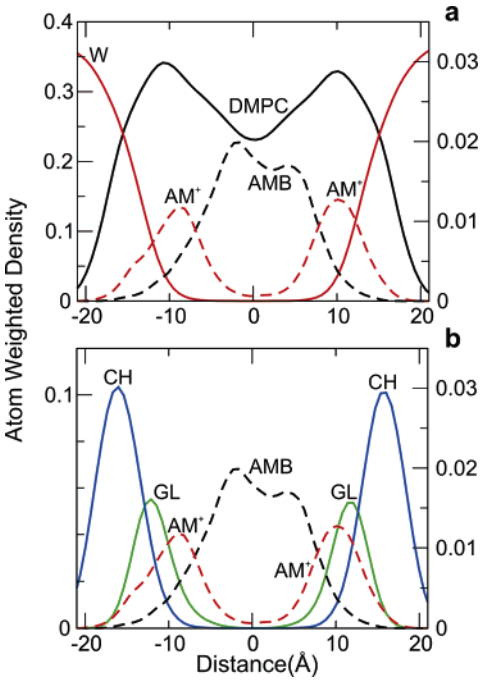

Figure 5. Atom weighted densities for the lipid bilayer (solid lines) and the AM molecules (dashed lines) for simulations with 0 (black), 2 (red), 8 (green), and 18 (blue) antimicrobial molecules. The scale on the left corresponds to the lipid molecules, while the scale on the right corresponds to the AM polymers.

effect is exacerbated with increasing AM concentration and has been noted previously for melittin penetration into a lipid bilayer.[31] However, the asymmetry between the pure inner leaflet and the AM containing outer leaflet may be exaggerated due to finite size effects, which in turn can enhance water penetration into the leaflet opposite to the AM attack.

In the absence of AM molecules in the bilayer, water can spontaneously diffuse past the lipid headgroups but is normally expelled back into the bulk region. The presence of AM molecules within both bilayer leaflets allows for occasional AM alignment perpendicular to the bilayer plane, thereby providing a stepping-stone pathway for water molecules to cross the membrane, as shown schematically in Figure 6. In this figure, snapshots of a single water molecule are taken during a passage across the membrane. The lipid bilayer and the surrounding water molecules have been abstracted into color panels for clarity. The water approaches from the water subphase and crosses the lipid headgroup region, where it finds an antimicrobial molecule. At this stage, the water unit interacts with the hydrophilic site until the bottom AM molecule aligns properly. At this time a quick jump occurs between both molecules, and the water now resides in the lower leaflet. The water finally crosses the lower leaflet headgroup region and returns to the water subphase.

In effect, water or ions could become transiently bound within the core of the bilayer by the hydrophilic groups of the AM. Thermal fluctuations can drive this bound water deeper into the membrane whereupon it can jump to an appropriately positioned AM in the opposite leaflet and eventually exit the membrane after crossing the bilayer core.

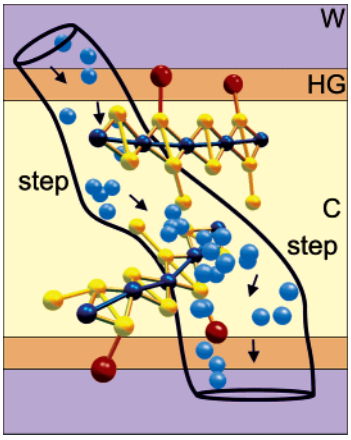

Figure 6. Representative water trajectories (blue spheres are CG waters) showing passage from the bulk water phase, W1 (purple), through the headgroup region HG1 (orange), and hydrophobic membrane core, C (yellow) to the HG2 and W2 regions via a pathway employing the aryl amide molecules as stepping stones.

The observed water transport is a rare event for a system of this size and even for a simulation of this length. In the highest concentration simulation, the water molecule passage rate is roughly 1/ns, which is about three times that of the pure CG membrane. This type of ion or water transport has been suggested as a viable mechanism for the function of hydraphile channels.[32] It is important to note that our water unit represents three loosely packed water molecules. As such, it is also comparable to a hydrated ion. This suggests that hydrated ions could gain passage through the bilayer by means of this mechanism. It is important to note that these water-passage results across the membrane are to be taken in a slightly qualitative manner as the coarse grain representation of the units interacting here does not allow for a more quantitative description of the passage event. It is clear, however, that the presence of the antimicrobials, mediating the water passage, results in an increase in the overall water-passage rate.

Conclusion

We see no evidence for the formation of pores when these synthetic AMs oligomerize during attack on the membrane and subsequently undergo trans-bilayer flips. This lack of pore formation could be due, at least in part, to the fact that the AMs are too short to span the bilayer.[12] However, interactions between AMs are fundamental for the disruption of the lipid bilayer. As such, these results emphasize AM cooperativity which is integral to the traditional Shai-Matsuzaki-Huang model and provides an alternative mechanism for transport across the membrane. This molecular level simulation of the interfacial insertion and penetration process suggests a possible new approach to generate targets drugs for pathogen eradication. The present results are not aimed to dispute the compelling evidence that exists regarding nanopore formation by natural AMs, rather they provide a basis for the design of low-cost synthetic AM molecules which could disrupt a cellular membrane through an alternative pathway.

The traditionally accepted mechanism for water transport involves the formation of pores by amphiphilic peptides. Here, however, the AMs, rather than forming a pore, provide a local hydrophilic environment to trap water within the globally hydrophobic membrane core. At high AM concentrations the probability for the alignment of AMs in opposite leaflets to form a bridge across the bilayer is increased. This suggests a previously unexplored pathway for membrane leakage and poration. Furthermore, in a fully atomistic environment, the formation of water wires across the bilayer seems plausible.[33,34] From our results we see that pore formation may not be necessary and that if AM bilayer flips can occur, water leakage is possible.

The efficiency of the aryl amide class of AMs, their ease of synthesis, and, as shown in this paper, their specific interaction with the membrane provides thought-provoking insight into possible AM design. The presented observations also provide an explanation of the fundamental interactions between generic amphiphilic molecules and lipid membranes. The present study presents researchers with a qualitative picture of the mode of action of a purely synthetic AM polymer which can be generalized to generic models and thus should be able to impact in the design of new and more potent antimicrobial agents.

Acknowledgment. This research was supported by generous grants from the National Institutes of Health (NIH). The authors thank Preston Moore, Bin Chen, Robert Doerksen, and Dahui Liu (PolyMedix) for discussions and important insights. C.F.L. would like to thank Richard Darst for assistance during the writing of this manuscript.

Note Added after ASAP Publication. This paper was released ASAP on March 24, 2006, with the incorrect Received Date. The correct version was posted on April 12, 2006.

References

(1) Brower, V. *EMBO Rep.* **2003,** *4*, 649−651.

(2) Cohen, M. L. *Nature* **2000**, *406*, 762−767.

(3) Anderson, R. M. *Nature Med.* **1999**, *5*, 147−149.

(4) Niller, E. *Nature Biotechnol.* **2002**, *20*, 21−25.

(5) Fernandez-Lopez, S.; Kim, H. S.; Choi, E. C.; Delgado, M.; Granja, J. R.; Khasanov, A..; Kraehenbuehl, K.; Long, G.; Weinberger, D. A.; Wilcoxen, K. M.; Ghadiri, M. R. *Nature* **2001**, *412*, 452−455.

(6) Zasloff, M. *Nature* **2002**, *415*, 389−395.

(7) Yang, L.; Harroun, T. A.; Weiss, M.; Ding, L.; Huang, H. W. *Biophys. J.* **2001**, *81*, 1475−1485.

(8) Bailey, H. *Curr. Opin. Biotech.* **1999**, *10*, 94−103.

(9) Lear, J. D.; Gratkowski, H. L.; DeGrado, W. F. *Biochem. Soc. T.* **2001**, *29*, 559−564.

(10) Raguse, T. L.; Porter, E. A.; Weisblum, B.; Gellman, S. H. *J. Am. Chem. Soc.* **2002**, *124*, 12774−12785.

(11) Patch, J. A.; Barron, A. E. *J. Am. Chem. Soc.* **2003**, *25*, 12092−12093.

(12) Tew, G. N.; Liu, D. H.; Chen, B.; Doerksen, R. J.; Kaplan, J.; Carroll, P. J.; Klein, M. L.; DeGrado, W. F. *Proc. Natl. Acad. Sci. U.S.A.* **2002**, *99*, 5110−5114.

(13) Shai, Y. *Biopolymers* **2002**, *66*, 236−248.

(14) Matsuzaki, K. *Biochim. Biophys. Acta*, **1999**, *1462*, 1−10.

(15) Allen, N. E.; Nicas, T. I. *FEMS Microbiol. Rev.* **2003**, *26*, 511−532.

(16) Although glycopeptide antibiotics such as vancomycin have membrane activity, their efficacy relies on the inhibition of the production of bacterial peptidoglycan for cell wall maintenance.

(17) Porter, E. A.; Wang, X. F.; Lee, H. S.; Weisblum, B.; Gellman, S. H. *Nature* **2000**, *404*, 565−565.

(18) Daggett V.; Fersht, A. *Nat. Rev. Mol. Cell Biol.* **2003**, *4*, 497−502.

(19) Jensen, M. Ø.; Park, S.; Tajkhorshid, E.; Schulten, K. *Proc. Natl. Acad. Sci. U.S.A.* **2002**, *99*, 6731−6736.

(20) La Rocca, P.; Shai, Y.; Sansom, M. S. P. *Biophys. Chem.* **1999**, *76*, 145−159.

(21) Aliste, M. P.; MacCallum, J. L.; Tieleman, D. P. *Biochemistry* **2003**, *42*, 8976−8987.

(22) Karaborni, S.; Esselink, K.; Hilbers, P.; Smit, B.; Karthauser, J.; Vanos, N.; Zana, R. *Science* **1994**, *266*, 254−256.

(23) Shelley, J. C.; Shelley, M. Y.; Reeder, R. C.; Bandyopadhyay, S.; Klein, M. L. *J. Phys. Chem. B* **2001**, *105*, 4464−4470.

(24) Izvekov S.; Voth G. A. *J. Phys. Chem. B* **2005**, *109*, 2469−2473.

(25) Lopez, C. F.; Moore, P. B.; Shelley, J. C.; Shelley, M. Y.; Klein, M. L. *Comput. Phys. Commun.* **2002**, *147*, 1−6.

(26) Kale, L.; Skeel, R.; Bhandarkar, M.; Brunner, R.; Gursoy, A.; Krawetz, N.; Phillips, J.; Shinozaki, A.; Varadarajan, K.; Schulten, K. *J. Comput. Phys.* **1999**, *151*, 283−312.

(27) Nielsen, S. O.; Lopez, C. F.; Srinivas, G.; Klein, M. L. *J. Phys.: Condens. Matter* **2004**, *16*, R481−R512.

(28) Tuckerman, M. J.; Berne, B. J.; Martyna, G. J. *J. Chem. Phys.* **1992**, *97*, 1990−2001.

(29) Moore, P. B.; Klein, M. L. *Implementation of a General Integration for Extended System Molecular Dynamics*; Technol. Report; University of Pennsylvania, 1997. http://www.cmm.upenn.edu/moore/code/code.html.

(30) Chen, F. Y.; Lee, M. T.; Huang, H. W. *Biophys. J.* **2003**, *84*, 3751−3758.

(31) Berneche, S.; Nina, M.; Roux, B. *Biophys. J.* **1998**, *75*, 1603−1618.

(32) Leevy W. M.; Donato, G. M.; Ferdani, R.; Goldman, W. E.; Schlesinger, P. H.; Gokel, G. W. *J. Am. Chem. Soc.* **2002**, *124*, 9022−9023.

(33) Tepper, H. L.; Voth, G. A. *Biophys J.* **2005**, *88*, 3095−3108.

(34) Decoursey, T. E. *Physiol. Rev.* **2003**, *83*, 475−579.

CT050298P